Looking closer at acute respiratory distress syndrome: the role of advanced imaging techniques

Giacomo Bellani[a,b], *Jean-Jaques Rouby*[c], *Jean-Michel Constantin*[d], *and Antonio Pesenti*[e]

Purpose of review
Advanced imaging techniques have provided invaluable insights in understanding of acute respiratory distress syndrome (ARDS) and the effect of therapeutic strategies, thanks to the possibility of gaining regional information and moving from simple 'anatomical' information to in-vivo functional imaging.

Recent findings
Computed tomography (CT) led to the understanding of several ARDS mechanisms and interaction with mechanical ventilation. It is nowadays frequently part of routine diagnostic workup, often leading to treatment changes. Moreover, CT is a reference for novel techniques both in clinical and preclinical studies. Bedside transthoracic lung ultrasound allows semiquantitative regional analysis of lung aeration, identifies ARDS lung morphology and response to therapeutic maneuvers. Electrical impedance tomography is a radiation-free, functional, bedside, imaging modality which allows a real-time monitoring of regional ventilation. Finally, positron emission tomography (PET) is a functional imaging technique that allows to trace physiologic processes, by administration of a radioactive molecule. PET with ^{18}FDG has been applied to patients with ARDS, thanks to its ability to track the inflammatory cells activity.

Summary
Progresses in lung imaging are key to individualize therapy, diagnosis, and pathophysiological mechanism at play in any patient at any specified time, helping to move toward personalized medicine for ARDS.

Keywords
acute respiratory distress syndrome, computed tomography, electrical impedance tomography, imaging, lung ultrasounds, positron emission tomography

INTRODUCTION

Acute respiratory distress syndrome (ARDS) is a relatively frequent and still often lethal disease [1▪]. Although a plain chest X-ray is sufficient to diagnose ARDS [2], more advanced imaging techniques have provided invaluable insights in our understanding of the disease and the effect of therapeutic strategies [3▪▪]. The role of imaging in ARDS is crucial for, at least, two reasons. The first one is the possibility of gaining regional information, which is particularly appealing in the context of a heterogeneous disease. A classical example is the balance between alveolar recruitment and overdistension, in response to a change of positive end-expiratory pressure [4]. Second, modern techniques allow imaging, *in vivo*, not exclusively of anatomical structures but of functions. In the present review, we summarize the most recent reports concerning imaging studies in ARDS. For clarity purposes, the review has been organized according to the different techniques. Even if very

[a]Department of Medicine and Surgery, University of Milan-Bicocca, [b]Department of Emergency and Intensive Care, San Gerardo Hospital, Monza, Italy, [c]Multidisciplinary Intensive Care Unit, Department of Anesthesia and Critical Care, Pitie-Salpêtrière Hospital, Assistance Publique Hopitaux de Paris, University School of Medicine Pierre and Marie Curie, UPMC (University Paris-6), Paris, [d]Intensive Care Unit, Department of Perioperative Medicine, University Hospital of Clermont-Ferrand, Centre Hospitalo-Universitaire de Clermont-Ferrand, Clermont Université, Université d'Auvergne, France and [e]Dipartimento di Anestesia, Rianimazione ed Emergenza Urgenza, Fondazione IRCCS Cà Granda-Ospedale Maggiore Policlinico and Dipartimento di Fisiopatologia Medico-Chirurgica e dei Trapianti, Università degli Studi di Milano, Milan, Italy

Correspondence to Antonio Pesenti, Dipartimento di Anestesia, Rianimazione ed Emergenza Urgenza, Fondazione IRCCS Cà Granda-Ospedale Maggiore Policlinico Dipartimento di Fisiopatologia Medico-Chirurgica e dei Trapianti, Università degli Studi di Milano, Via F. Sforza 35, 20122 Milano, Italy. Tel: +39 02 5503 3232; fax: +39 02 5503 3230; e-mail: antonio.pesenti@unimi.it

Curr Opin Crit Care 2017 23:000–000
DOI:10.1097/MCC.0000000000000380

KEY POINTS

- Imaging techniques provided unique understanding in the pathophysiology of ARDS and the role of mechanical ventilation.
- CT is nowadays part of routine diagnostic workup of several cases and remains the reference for novel techniques both in clinical and preclinical studies.
- Electrical impedance tomography allows bedside, continuous, real-time, and quantitative imaging of ventilation.
- Bedside transthoracic lung ultrasound allows semiquantitative regional analysis of lung aeration, identifies ARDS lung morphology, and response to therapeutic maneuvers.

promising for lung functional imaging, we will not focus on magnetic resonance, because its application to ARDS remain relatively rare and confined to preclinical field [5▪▪,6,7].

COMPUTED TOMOGRAPHY

Over the last three decades, CT has been one of the cornerstones in the understanding of ARDS mechanisms and of mechanical ventilation role in modulating lung regional aeration [8,9]. CT scan is nowadays part of routine clinical diagnostic workup of several ARDS cases [10▪▪,11]. A large retrospective study evaluated the findings of 204 CT scans obtained in patients with ARDS [12]. These led to a change in treatment strategy in about one quarter of cases and, interestingly, patients in whom therapeutic strategy was modified had a lower mortality than the rest of the cohort. Transportation for CT scan appeared well tolerated. It was associated with an 8.3% rate of complications, but all patients recovered to their baseline level returning to the ICU [12]. Burnham *et al.* [13] analyzed high-resolution CT scans obtained at day 14 since ARDS diagnosis, looking for signs of fibroproliferative activity, such as reticulation, ground glass opacification, and bronchiectasis, showing an association between these signs and diminished compliance of the respiratory system. In an elegant follow-up study [14], investigating ARDS survivors at 5 years, CT abnormalities were frequent (75% of the subjects) but minor. No relationship was found between CT abnormalities and functional alterations. Interestingly, these abnormalities were located in the nondependent regions, that is those more exposed to high ventilatory pressures and FiO_2 [14,15]. To limit the amount of radiation exposure for the patients, the possibility of using a low radiation exposure protocol appears promising [16], particularly for longitudinal follow-up or for assessment of lung recruitability at different airway pressures. Another limitation of performing quantitative CT scans analysis is the need to separate lung parenchyma from the surrounding tissues. Automated algorithms are usually not applicable to the ARDS lungs, which show extensive aeration loss. To this end, a semiautomatic method for segmentation has been developed and tested in rats with acute lung injury. The model showed a good performance when compared to expert human observers [17], albeit a validation in patients is still required.

Besides this clinical application, CT remains an invaluable tool to investigate ARDS mechanisms and the role of mechanical ventilation, as well as a reference for novel methods/techniques, as shown by several studies, focused on lung inhomogeneity [18,19▪], alveolar recruitment [20,21], and regional perfusion [22].

ULTRASOUND

Bedside transthoracic lung ultrasound has deeply changed lung imaging in the ICU. Like CT, it allows a regional analysis of lung aeration and identifies ARDS lung morphology (focal vs. diffuse aeration loss) [23]. It accurately assesses lung aeration changes following positive end-expiratory pressure (PEEP) [24], prone position [25], drainage of large pleural effusions [26], and administration of antibiotics in ventilator-associated pneumonia [27].

Each intercostal space, which offers an acoustic window toward the lung, has to be examined [28]. The normally aerated parenchyma is not visible because ultrasounds are not transmitted through organs filled with gas. Beyond the subcutaneous tissue, the pleural line is identified, with its characteristic lung sliding caused by inspiratory/expiratory movements of parietal and visceral pleural layers on each other. Beyond the pleura, multiple parallel horizontal A lines are identified, representing artefactual repetitions of the pleural line. When pulmonary inflammation, interstitial fibrosis, or lung edema decrease lung aeration, the lung parenchyma is still not visible because of the persistence of gas in the alveolar space. However, artefactual vertical B lines appear, resulting from the abnormal interface between pulmonary gas and increased lung tissue. Their distribution and characteristics (number, spacing, origin) serve to identify interstitial edema, interstitial pneumonia, lung fibrosis, and alveolar edema (cardiogenic or high permeability). Multiple spaced B lines correspond to moderate aeration loss whereas coalescent and extended B lines correspond

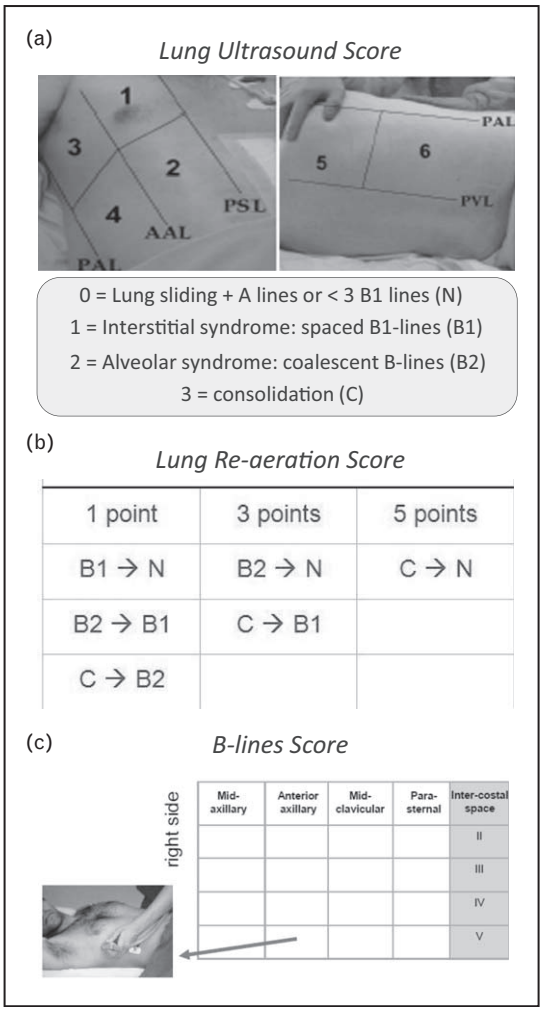

FIGURE 1. Ultrasound scores for quantifying lung aeration loss and its variations. (a) Lung ultrasound score quantifies aeration loss in acute respiratory distress syndrome (ARDS). Six regions of interest are examined on each side, delineated by parasternal line (PSL), anterior axillary line (AA), posterior axillary line (PAL), paravertebral line, and mid-mammillary line: upper and lower anterior, lateral and posterior lung regions (1–6). Each intercostal space of each region (the acoustic window to the lung parenchyma) is examined. Upper and lower anterior regions and upper lateral region are characterized aeration, 1 = moderate loss of aeration, 2 = severe loss of aeration, and 3 = complete aeration loss. The evaluation is made on both sides and the lung ultrasound score is calculated as the sum of numbers characterizing the 12 examined regions. The lung ultrasound score varies from 0 to 36. Modified from [28,29] (original). (b) Lung re-aeration score allows to quantify re-aeration resulting from different therapies: positive end-expiratory pressure (PEEP) in ARDS, drainage of massive pleural effusion, or antibiotic treatment for ventilator-associated pneumonia. Each region of interest is examined at two different PEEP levels or before or after pleural effusion drainage or antibiotic treatment. For a given region of interest, the change of aeration is evaluated as follows: a slight re-aeration (spaced B1 lines to A lines, coalescent B2 lines to spaced B1 lines, consolidation to coalescent B2 lines) is quoted 1 point; a substantial re-aeration (coalescent B2 lines to A lines, consolidation to spaced B1 lines) is quoted three points; a complete re-aeration (consolidation to A lines) is quoted five points. The re-aeration score is calculated as the sum of numbers characterizing the 12 examined regions. Re-aeration is considered as significant for re-aeration scores above 4 (data from 24). (c) B-lines score quantifies aeration loss in pulmonary edema (cardiogenic or high-permeability type). Eight regions of interest are examined on each side, delineated by parasternal, mid-clavicular, anterior and mid-axillary axillary lines. In each intercostal space, the number of B-lines is quantified (coalescent B2 lines = 10). The B-line score is calculated as the sum of numbers in each examined intercostal space. A score less than 5 indicates no pulmonary edema; a score between 6 and 15 indicates mild degree of pulmonary edema; a score between 16 and 30 indicates moderate degree of pulmonary edema; a score above 30 indicates severe degree of pulmonary edema. Modified with permission from [32].

to severe aeration loss. When there is no more gas into the respiratory system (tumors, pulmonary infarction, lung contusion, obstructive atelectasis, consolidation), then ultrasounds are transmitted through tissue structures and pulmonary lobes and segments, aorta, pulmonary vessels and bronchi become visible. The loss of lung aeration is complete. Ultrasound characteristics of consolidations (static and dynamic bronchogram, blood flow profile in pulmonary vessels, pleural effusion) serve to identify lung and pleural tumors, pulmonary infarction, inflammatory consolidations, lobar or segmental pneumonia, and lung abscesses. Consolidations are visible only when they extend to the parietal pleura. A consolidation surrounded by alveolar gas is not visible using transthoracic ultrasound. Interpretation and diagnostic values of ultrasound patterns have been extensively described [28]. Illustrative videos can be visualized and downloaded freely by connecting at http://www.reapitie-univparis6.aphp.fr.

A complete examination of both lungs takes approximately 10 min. The lung is divided in six regions on each sides: anterior-superior, anterior-inferior, lateral-superior, lateral-inferior, posterior-superior, and posterior-inferior. In the posterior-superior region, the acoustic window is limited to the intercostal spaces located between the paravertebral line and the internal limit of the scapula. In spontaneously breathing patients, positioning the patient's hands above the head increases the acoustic window. Intra- and interobserver reproducibility

is high, around 97%. The learning curve is short, varying from 3 weeks to 3 months and based on the achievement of 25 to 30 supervised ultrasound examinations. In ARDS, lung ultrasound is much more accurate than auscultation or bedside chest radiography to identify alveolar-interstitial syndrome, lung consolidation, pleural effusion, and pneumothorax [28,29]. In 15–20% of patients, the acoustic window is restricted (obesity, thoracic dressings, subcutaneous emphysema), rendering hazardous the interpretation of ultrasound findings.

In ARDS, lung ultrasound allows a semiquantitative assessment of lung aeration and its regional distribution. Because it is noninvasive and easily repeatable at the bedside, it accurately monitors lung aeration changes following PEEP [24], drainage of large pleural effusion [26], antimicrobial treatment of ventilator-associated pneumonia [27], negative or positive fluid balance [30]. For quantifying changes in lung aeration, three different scores have been proposed: lung aeration score (Fig. 1A) quantifies the lung aeration loss in ARDS [30] or during a spontaneous breathing trial [31]; lung re-aeration score (Fig. 1B) quantifies lung recruitment following PEEP in ARDS [2] and re-aeration following antibiotic treatment in ventilator-associated pneumonia [5▪▪]; B-line score quantifies the extension of aeration loss in pulmonary edema (Fig. 1C) [32] allowing the monitoring of extravascular lung water [33] and treatment efficiency [32].

Another potential benefit of bedside lung ultrasound is to characterize easily lung morphology [23]. As illustrated in Fig. 2, lung ultrasound is able to differentiate focal ARDS, characterized by a massive loss of aeration predominating in dependent parts of the lung ('black and white' lungs) from diffuse ARDS, characterized by a diffuse loss of aeration observed in all lung regions ('white' lungs). Recent data demonstrate that focal and diffuse ARDS are two different phenotypes that may require different therapeutic management [34,35▪]. Diffuse ARDS has a higher mortality, a higher rate of sepsis and expresses higher systemic levels of soluble advanced glycation end-products (sRAGE), protein S100A12, high-mobility group box-1 protein (HMGB1), and plasminogen activator inhibitor-1 (PAI-1). Elevated plasma sRAGE, a strong biomarker of epithelial injury, is associated to impaired alveolar fluid clearance [36,37] and distinct responses to ventilator strategy. The ongoing multicenter randomized controlled LIVE study should indicate whether ventilator setting should be adapted to sRAGE phenotype and ultrasound-based morphology in patients with ARDS (ClinicalTrials.gov identifier: NCT02149589).

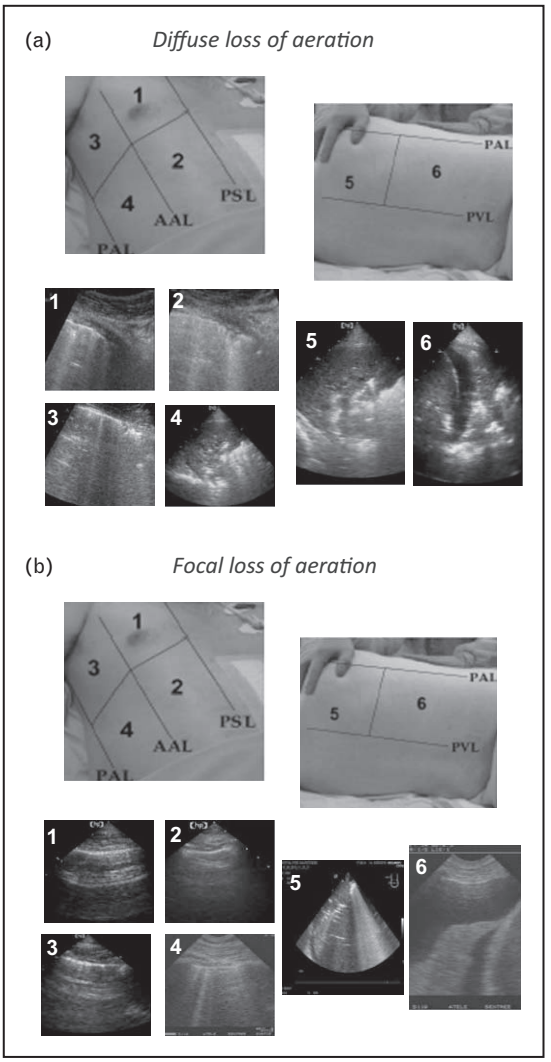

FIGURE 2. Lung ultrasound allows immediate characterization of lung morphology in acute respiratory distress syndrome (ARDS). (a) ARDS characterized by diffuse lung morphology. At PEEP 5 cmH_2O, right anterior and upper lateral regions (1–3) are characterized by coalescent B-lines (severe loss of aeration) whereas right lower lateral and posterior regions (4–6) are characterized by consolidation and pleural effusion (complete loss of aeration). Similar patterns are observed in the left side. There are no normally aerated lung regions: aeration loss concerns all lung regions. (b) ARDS characterized by focal lung morphology. At PEEP 5 cmH_2O, right anterior and lateral regions (1–4) are characterized by A-lines or less than three B-lines (normal aeration) whereas right posterior regions (5,6) are characterized by consolidation and pleural effusion (complete loss of aeration). Similar patterns are observed in the left side. Aeration loss predominates in posterior and dependent lung regions.

ELECTRICAL IMPEDANCE TOMOGRAPHY

Electrical impedance tomography (EIT) is a radiation-free, functional, bedside, imaging modality,

which allows a continuous a real-time monitoring of regional ventilation in a section of the chest. Although this technique has been described several years ago, the recent availability of different commercial devices has rapidly increased the interest of clinicians and researchers in this tool. The TRanslational EIT developmeNt stuDy group has recently published a consensus paper, which recapitulates experts' recommendations on data analysis, terminology, and clinical use [38▪▪]. Briefly, EIT can provide two types of information, both at a regional level: the amount of tidal ventilation reaching a given region and the changes in end expiratory lung impedance (reflecting the changes in end-expiratory lung volume) caused by changes in ventilatory settings. Although EIT is frequently assimilated to CT, it is important to underline that the two techniques provide quite substantially different information: CT offers images on lung aeration (unless sequential or dynamic scans are obtained) and EIT provides images of ventilation (i.e. on the dynamic changes in local aeration).

EIT has been extensively applied in preclinical studies, showing its ability to track alveolar recruitment and overdistension. At the same time, a growing number of publications show the value of EIT in clinical practice. Cinnella *et al.* applied EIT to assess the effects of an open lung approach strategy (based on recruitment maneuver and decremental PEEP). This ventilatory strategy allowed a more homogeneous distribution of tidal ventilation. The increased ventilation to dorsal regions was correlated with the improvement of arterial oxygenation [39▪]. In a group of patients with ARDS [40], Mauri *et al.* showed that a greater activation of the diaphragm, caused by the reduction of pressure support, was able to promote a more homogeneous distribution of ventilation (Fig. 3). The same group investigated the effect of periodic hyperinflation (sighs) on the regional strain: increasing the rate of sighs delivered (from 0.5 to 2 min^{-1}) led to higher end-expiratory lung volume, without causing increased overdistension [41].

Taking advantage of the very high temporal resolution of EIT, Yoshida *et al.* assessed the effects of a strenuous spontaneous breathing effort in an animal model of lung injury and in patients with ARDS. Notwithstanding identical global tidal

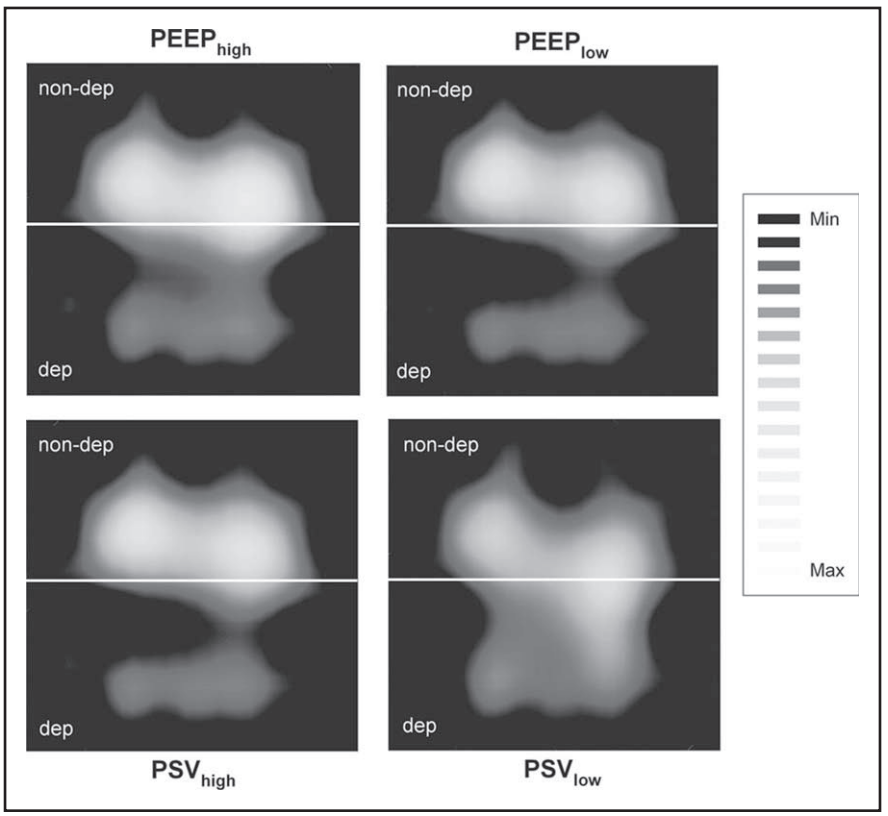

FIGURE 3. Electrical impedance tomography image reconstruction of regional ventilation (black = no ventilation, white = maximum ventilation in arbitrary scale) from one patient recovering from acute respiratory distress syndrome. Increased positive end-expiratory pressure (PEEP, top two images) and decreased pressure support (PSV, bottom two images) induced redistribution of tidal ventilation from nondependent (non-dep) to dependent (dep) lung regions. Reproduced with permission from [40].

volumes, the strenuous contraction of the diaphragm caused a redistribution of gas from non-dependent to dependent lung regions (pendelluft), which were hence subject to a regional overdistension [42].

A very promising feature of EIT, still requiring major developments and validation, resides in its potential to image lung regional perfusion, based on a bolus of hypertonic saline (which transiently decreases regional impedance in dependence of perfusion) [43] or the cardiac related impedance changes because of the blood flow pulsatility in small vessels [44].

POSITRON EMISSION TOMOGRAPHY

Positron emission tomography (PET) is a functional imaging technique that allows to trace a given physiological process, following the administration of a radioactively-labeled molecule. PET with [18F]fluoro-2-deoxy-D-glucose (^{18}FDG) has been applied to patients with ARDS, thanks to its ability to track the activity of inflammatory cells [45,46]. In patients with ARDS, PET provided direct evidence that lung inflammation affects also the regions which appear normally-aerated on CT scan [47]. Moreover, the inflammation of normally aerated lung was positively correlated with plateau pressure (with a steep increase above 27 cmH_2O) and with the ratio of tidal volume over end-expiratory lung volume (i.e. the 'dynamic strain') [48]. On the contrary, the regions undergoing tidal recruitment and derecruitment did not show signs of increased inflammation. These results were corroborated in an animal model of ARDS, where, for comparable tidal volume and driving pressure, volutrauma led to higher levels of inflammation than atelectrauma [49] did. More recently Cressoni *et al.* [50] combined sophisticated CT and PET analysis to demonstrate the tight association between lung heterogeneity and inflammation.

PET has also been extensively used in preclinical studies, to show the interplay between mechanical ventilation and other inflammatory stimuli [51▪,52]. One of these studies suggested that the increase in ^{18}FDG uptake can precede radiological and gas exchange abnormalities. For this reason, the authors propose that PET with ^{18}FDG could be an early biomarker in ARDS [53].

The aforementioned studies share the limitation that the ^{18}FDG signal lacks specificity for the inflammatory cells, being rather a sensitive marker of metabolic activity. The possibility of using a labeled ligand of vascular adhesion protein has been recently proposed as a mean to image the distribution of this adhesion molecule, expressed by endothelial cells in response to inflammatory stimuli. This tracer was tested in a porcine model of ARDS [54]: the detection of inflammation was feasible, but required additional procedures, including perfusion data obtained from [^{15}O]water, somewhat limiting the possibilities of using this tracer in clinical practice.

CONCLUSION

Progresses in lung imaging represent a major advance in ARDS since its original description in 1967. In the last few years, the role of computerized tomography and PET has been refined in both the clinical management and the pathophysiology of the syndrome. In the meantime, ultrasound has gained a capital role at the patient's bedside, and has become a fundamental technique to be mastered by any intensivist. EIT is a monitoring tool that allows the bedside continuous visualization of ventilation, aeration and tidal volume topographic distribution, with some promises about the possible visualization of lung perfusion. We have gone a long way from plain bedside chest X-ray, which nevertheless still constitutes a fundamental element of the diagnosis. Progresses in lung imaging are a fundamental tool in individualizing therapy, diagnosis, and pathophysiological mechanism at play in any patient at any specified time. Progress in lung imaging will help intensive care moving toward personalized medicine for patients with ARDS.

Acknowledgements

None.

Financial support and sponsorship

This work was supported by the Department of Medicine and Surgery, University of Milan-Bicocca, Milan, Italy.

Conflicts of interest

G.B. received lecturing fees and support for research from Draeger Medical, Lubeck, Germany. J.-J.R. and J.-M.C. have no COI to declare. A.P. received Honoraria from Baxter, Boehringer Ingelheim and grant from Novalung, outside the scope of this work.

REFERENCES AND RECOMMENDED READING

Papers of particular interest, published within the annual period of review, have been highlighted as:

- ▪ of special interest
- ▪▪ of outstanding interest

1. Bellani G, Laffey JG, Pham T, *et al.* Epidemiology, patterns of care, and ▪ mortality for patients with acute respiratory distress syndrome in intensive care units in 50 countries. JAMA 2016; 315:788–800.

Observational worldwide study, focused on ARDS management including more than 3000 patients with ARDS.

2. Ranieri VM, Rubenfeld GD, Thompson BT, *et al.* Acute respiratory distress syndrome: the Berlin Definition. JAMA 2012; 307:2526–2533.
3. ■■ Pesenti A, Musch G, Lichtenstein D, *et al.* Imaging in acute respiratory distress syndrome. Intens Care Med 2016; 42:686–698.

State of the art review with also an historical overview on the role of imaging in ARDS.

4. Costa EL, Borges JB, Melo A, *et al.* Bedside estimation of recruitable alveolar collapse and hyperdistension by electrical impedance tomography. Intens Care Med 2009; 35:1132–1137.
5. ■■ Cereda M, Xin Y, Hamedani H, *et al.* Mild loss of lung aeration augments stretch in healthy lung regions. J Appl Physiol 2016; 120:444–454.

Elegant preclinical study showing, by hyperpolarized gas MRI, how aeration loss can expose aerated lung regions to increased risk of injury from ventilation.

6. Cereda M, Xin Y, Kadlecek S, *et al.* Hyperpolarized gas diffusion MRI for the study of atelectasis and acute respiratory distress syndrome. NMR Biomed 2014; 27:1468–1478.
7. Kobayashi N, Lei J, Utecht L, *et al.* 3D cine magnetic resonance imaging of rat lung ARDS using gradient-modulated SWIFT with retrospective respiratory gating. Proc SPIE Int Soc Opt Eng 2015; pii:941718.
8. Gattinoni L, Caironi P, Pelosi P, Goodman LR. What has computed tomography taught us about the acute respiratory distress syndrome? Am J Respir Crit Care Med 2001; 164:1701–1711.
9. Rouby JJ, Puybasset L, Nieszkowska A, Lu Q. Acute respiratory distress syndrome: lessons from computed tomography of the whole lung. Crit Care Med 2003; 31 (4 Suppl):S285–S295.
10. ■■ Papazian L, Calfee CS, Chiumello D, *et al.* Diagnostic workup for ARDS patients. Intens Care Med 2016; 42:674–685.

Elegant review article which recapitulates the diagnostic workup recommended for ARDS, with different techniques.

11. Gibelin A, Parrot A, Maitre B, *et al.* Acute respiratory distress syndrome mimickers lacking common risk factors of the Berlin definition. Intens Care Med 2016; 42:164–172.
12. Simon M, Braune S, Lagmani A, *et al.* Value of computed tomography of the chest in subjects with ARDS: a retrospective observational study. Respir Care 2016; 61:316–323.
13. Burnham EL, Hyzy RC, Paine R 3rd, *et al.* Detection of fibroproliferation by chest high-resolution CT scan in resolving ARDS. Chest 2014; 146:1196–1204.
14. Wilcox ME, Patsios D, Murphy G, *et al.* Radiologic outcomes at 5 years after severe ARDS. Chest 2013; 143:920–926.
15. Nieszkowska A, Lu Q, Vieira S, *et al.* Incidence and regional distribution of lung overinflation during mechanical ventilation with positive end-expiratory pressure. Crit Care Med 2004; 32:1496–1503.
16. Vecchi V, Langer T, Bellomi M, *et al.* Low-dose CT for quantitative analysis in acute respiratory distress syndrome. Crit Care 2013; 17:R183.
17. Xin Y, Song G, Cereda M, *et al.* Semiautomatic segmentation of longitudinal computed tomography images in a rat model of lung injury by surfactant depletion. J Appl Physiol 2015; 118:377–385.
18. Cressoni M, Cadringher P, Chiurazzi C, *et al.* Lung inhomogeneity in patients with acute respiratory distress syndrome. Am J Respir Crit Care Med 2014; 189:149–158.
19. ■ Cereda M, Xin Y, Meeder N, *et al.* Visualizing the propagation of acute lung injury. Anesthesiology 2016; 124:121–131.

In this preclinical study, the spatial evolution of acid aspiration and ventilation induced lung injury is demonstrated by serial CT scans.

20. Derosa S, Borges JB, Segelsjo M, *et al.* Reabsorption atelectasis in a porcine model of ARDS: regional and temporal effects of airway closure, oxygen, and distending pressure. J Appl Physiol 2013; 115:1464–1473.
21. Garcia-Prieto E, Lopez-Aguilar J, Parra-Ruiz D, *et al.* Impact of recruitment on static and dynamic lung strain in acute respiratory distress syndrome. Anesthesiology 2016; 124:443–452.
22. Dakin J, Jones AT, Hansell DM, *et al.* Changes in lung composition and regional perfusion and tissue distribution in patients with ARDS. Respirology 2011; 16:1265–1272.
23. Bouhemad B, Mongodi S, Via G, Rouquette I. Ultrasound for 'lung monitoring' of ventilated patients. Anesthesiology 2015; 122:437–447.
24. Bouhemad B, Brisson H, Le-Guen M, *et al.* Bedside ultrasound assessment of positive end-expiratory pressure-induced lung recruitment. Am J Respir Crit Care Med 2011; 183:341–347.
25. Haddam M, Zieleskiewicz L, Perbet S, *et al.* Lung ultrasonography for assessment of oxygenation response to prone position ventilation in ARDS. Intens Care Med 2016; 42:1546–1556.
26. Chinardet B, Brisson H, Arbelot C, *et al.* Ultrasound assessment of lung consolidation and reaeration after pleural effusion drainage in patients with acute respiratory distress syndrome: a pilot study. Acta Anaesthesiol Belgica 2016; 67:29–35.
27. Bouhemad B, Liu ZH, Arbelot C, *et al.* Ultrasound assessment of antibiotic-induced pulmonary reaeration in ventilator-associated pneumonia. Crit Care Med 2010; 38:84–92.
28. Volpicelli G, Elbarbary M, Blaivas M, *et al.* International evidence-based recommendations for point-of-care lung ultrasound. Intens Care Med 2012; 38:577–591.
29. Lichtenstein D, Goldstein I, Mourgeon E, *et al.* Comparative diagnostic performances of auscultation, chest radiography, and lung ultrasonography in acute respiratory distress syndrome. Anesthesiology 2004; 100:9–15.
30. Caltabeloti F, Monsel A, Arbelot C, *et al.* Early fluid loading in acute respiratory distress syndrome with septic shock deteriorates lung aeration without impairing arterial oxygenation: a lung ultrasound observational study. Crit Care 2014; 18:R91.
31. Soummer A, Perbet S, Brisson H, *et al.* Ultrasound assessment of lung aeration loss during a successful weaning trial predicts postextubation distress. Crit Care Med 2012; 40:2064–2072.
32. Gargani L. Lung ultrasound: a new tool for the cardiologist. Cardiovasc Ultrasound 2011; 9:6.
33. Baldi G, Gargani L, Abramo A, *et al.* Lung water assessment by lung ultrasonography in intensive care: a pilot study. Intens Care Med 2013; 39:74–84.
34. Jabaudon M, Blondonnet R, Roszyk L, *et al.* Soluble forms and ligands of the receptor for advanced glycation end-products in patients with acute respiratory distress syndrome: an observational prospective study. PloS One 2015; 10:e0135857.
35. ■ Mrozek S, Jabaudon M, Jaber S, *et al.* Elevated plasma levels of sRAGE are associated with non-focal CT-based lung imaging in ARDS patients: a prospective multicenter study. Chest 2016; 150:998–1007.

This prospective multicenter study shows that the diffuse ARDS morphology (diffuse loss of lung aeration—'white lungs') is characterized by increased plasma levels of sRAGE, a biomarker of epithelial injury.

36. Jabaudon M, Blondonnet R, Roszyk L, *et al.* Soluble receptor for advanced glycation end-products predicts impaired alveolar fluid clearance in acute respiratory distress syndrome. Am J Respir Crit Care Med 2015; 192:191–199.
37. Jabaudon M, Blondonnet R, Lutz J, *et al.* Net alveolar fluid clearance is associated with lung morphology phenotypes in acute respiratory distress syndrome. Anaesth Crit Care Pain Med 2016; 35:81–86.
38. ■■ Frerichs I, Amato MB, van Kaam AH, *et al.* Chest electrical impedance tomography examination, data analysis, terminology, clinical use and recommendations: consensus statement of the TRanslational EIT developmeNt stuDy group. Thorax 2016. [Epub ahead of print]

State-of-the-art consensus conference on EIT.

39. ■ Cinnella G, Grasso S, Raimondo P, *et al.* Physiological effects of the open lung approach in patients with early, mild, diffuse acute respiratory distress syndrome: an electrical impedance tomography study. Anesthesiology 2015; 123:1113–1121.

In this crossover study, the effect of a decremental PEEP trial was studied in 15 patients with ARDS, under several aspects, including EIT.

40. Mauri T, Bellani G, Confalonieri A, *et al.* Topographic distribution of tidal ventilation in acute respiratory distress syndrome: effects of positive end-expiratory pressure and pressure support. Crit Care Med 2013; 41:1664–1673.
41. Mauri T, Eronia N, Abbruzzese C, *et al.* Effects of sigh on regional lung strain and ventilation heterogeneity in acute respiratory failure patients undergoing assisted mechanical ventilation. Crit Care Med 2015; 43:1823–1831.
42. Yoshida T, Torsani V, Gomes S, *et al.* Spontaneous effort causes occult pendelluft during mechanical ventilation. Am J Respir Crit Care Med 2013; 188:1420–1427.
43. Borges JB, Suarez-Sipmann F, Bohm SH, *et al.* Regional lung perfusion estimated by electrical impedance tomography in a piglet model of lung collapse. J Appl Physiol 2012; 112:225–236.
44. Mauri T, Eronia N, Turrini C, *et al.* Bedside assessment of the effects of positive end-expiratory pressure on lung inflation and recruitment by the helium dilution technique and electrical impedance tomography. Intens Care Med 2016; 42:1576–1587.
45. Zambelli V, Di Grigoli G, Scanziani M, *et al.* Time course of metabolic activity and cellular infiltration in a murine model of acid-induced lung injury. Intens Care Med 2012; 38:694–701.
46. Saha D, Takahashi K, de Prost N, *et al.* Micro-autoradiographic assessment of cell types contributing to 2-deoxy-2-[(18)F]fluoro-D-glucose uptake during ventilator-induced and endotoxemic lung injury. Mol Imag Biol 2013; 15:19–27.
47. Bellani G, Messa C, Guerra L, *et al.* Lungs of patients with acute respiratory distress syndrome show diffuse inflammation in normally aerated regions: a [18F]-fluoro-2-deoxy-D-glucose PET/CT study. Crit Care Med 2009; 37:2216–2222.
48. Bellani G, Guerra L, Musch G, *et al.* Lung regional metabolic activity and gas volume changes induced by tidal ventilation in patients with acute lung injury. Am J Respir Crit Care Med 2011; 183:1193–1199.
49. Guldner A, Braune A, Ball L, *et al.* Comparative effects of volutrauma and atelectrauma on lung inflammation in experimental acute respiratory distress syndrome. Crit Care Med 2016; 44:e854–e865.
50. Cressoni M, Chiumello D, Chiurazzi C, *et al.* Lung inhomogeneities, inflation and [18F]2-fluoro-2-deoxy-D-glucose uptake rate in acute respiratory distress syndrome. Eur Respir J 2016; 47:233–242.

51. Borges JB, Costa EL, Bergquist M, *et al.* Lung inflammation persists after 27 h of ■ protective acute respiratory distress syndrome network strategy and is concentrated in the nondependent lung. Crit Care Med 2015; 43:e123–e132.
Preclinical long-term study, reporting serial measurement of lung inflammation by PET.
52. Borges JB, Senturk M, Ahlgren O, *et al.* Open lung in lateral decubitus with differential selective positive end-expiratory pressure in an experimental model of early acute respiratory distress syndrome. Crit Care Med 2015; 43:e404–e411.
53. Wellman TJ, de Prost N, Tucci M, *et al.* Lung metabolic activation as an early biomarker of acute respiratory distress syndrome and local gene expression heterogeneity. Anesthesiology 2016; 125:992–1004.
54. Retamal J, Sorensen J, Lubberink M, *et al.* Feasibility of (68)Ga-labeled Siglec-9 peptide for the imaging of acute lung inflammation: a pilot study in a porcine model of acute respiratory distress syndrome. Am J Nuclear Med Mol Imag 2016; 6:18–31.